Robert Streubel Papers   Research Papers in Physics and Astronomy

9-24-2012

Equilibrium magnetic states in individual hemispherical permalloy caps

Robert Streubel
Leibniz-Institut für Festkörper- und Werkstoffforschung Dresden, streubel@unl.edu

Volodymyr P. Kravchuk
Bogolyubov Institute for Theoretical Physics Nasu

Denis D. Sheka
Taras Shevchenko National University of Kyiv

Denys Makarov
Leibniz-Institut für Festkörper- und Werkstoffforschung Dresden

Florian Kronast
Helmholtz-Zentrum Berlin für Materialien und Energie (HZB)

See next page for additional authors

Authors

Robert Streubel, Volodymyr P. Kravchuk, Denis D. Sheka, Denys Makarov, Florian Kronast, Oliver G. Schmidt, and Yuri Gaididei

Equilibrium magnetic states in individual hemispherical permalloy caps

Robert Streubel, Volodymyr P. Kravchuk, Denis D. Sheka, et al.

View Online **Export Citation**

ARTICLES YOU MAY BE INTERESTED IN
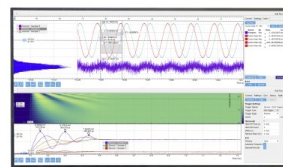
Equilibrium magnetic states in individual hemispherical permalloy caps

Robert Streubel,[1,2,a)] Volodymyr P. Kravchuk,[3] Denis D. Sheka,[4] Denys Makarov,[1] Florian Kronast,[5] Oliver G. Schmidt,[1,2] and Yuri Gaididei[3]

[1]*Institute for Integrative Nanosciences, IFW Dresden, 01069 Dresden, Germany*
[2]*Material Systems for Nanoelectronics, Chemnitz University of Technology, 09107 Chemnitz, Germany*
[3]*Bogolyubov Institute for Theoretical Physics, 03143 Kiev, Ukraine*
[4]*Radiophysics Faculty, Taras Shevchenko National University of Kiev, 01601 Kiev, Ukraine*
[5]*Helmholtz-Zentrum Berlin für Materialien und Energie GmbH, 12489 Berlin, Germany*

The magnetization distributions in individual soft magnetic permalloy caps on non-magnetic spherical particles with sizes ranging from 50 to 800 nm are investigated. We experimentally visualize the magnetic structures at the resolution limit of the x-ray magnetic circular dichroism photoelectron emission microscopy (XMCD-PEEM). By analyzing the so-called tail contrast in XMCD-PEEM, the spatial resolution is significantly enhanced, which allowed us to explore magnetic vortices and their displacement on curved surfaces. Furthermore, cap nanostructures are modeled as extruded hemispheres to determine theoretically the phase diagram of equilibrium magnetic states. The calculated phase diagram agrees well with the experimental observations. © *2012 American Institute of Physics.* [http://dx.doi.org/10.1063/1.4756708]

Topological effects in magnetic nanostructures have become very attractive to tune magnetic properties in a deterministic way. One of the most prominent examples is the appearance of topologically stabilized magnetic vortices in patterned magnetic films.[1,2] The magnetic vortex is characterized by two parameters, namely chirality (sense of curling of the in-plane magnetization) and polarity (orientation of the out-of-plane magnetic moment). The controlled creation and manipulation of these vortices are crucial for applications, such as magnetic logic and memory concepts.[3,4] Several approaches are introduced to tailor chirality and polarity of vortices that rely on either field-[5–7] or current-driven manipulation.[8–10] Very recently, we discovered in soft magnetic spherical shells that topology and curvature modify the in-surface structure of the vortex.[11] It is already known that curvature affects the magnetic properties of hard magnetic caps on spherical particles.[12,13] Both intercap exchange interaction and magnetization reversal exhibit substantial modifications with respect to their planar counterparts due to the curvature-driven thickness gradient. Curvature templates were also applied to prepare magnetic vortices in soft magnetic cap structures on spherical[14] and cylindrical objects,[15] which show a reduced magnetostatic intercap coupling. A chirality coupling between neighboring caps and novel chirality-frustrated states is observed in closely packed arrangements.[14] This coupling is expected to be strongly dependent on the thickness of the soft magnetic films and the size of the particles. In order to tailor the intercap interaction, the phase diagram (thickness-diameter) has to be explored for hemispherical cap structures in analogy to those for planar disks.[16]

In this work, we present the magnetization distributions in *individual* magnetic caps on non-magnetic spherical particles with sizes ranging from 50 to 800 nm. The magnetic structures are visualized at the resolution limit of the used x-ray magnetic circular dichroism photoelectron emission

microscope (XMCD-PEEM) set-up, which is of about 50 nm for curved magnetic samples.[15] By analyzing the so-called *tail contrast*, an enhanced spatial resolution is achieved, which is explored to study magnetic vortices and the displacement of the vortex cores. The origin of the tail contrast is elucidated. Micromagnetic simulations are carried out by using the full scale OOMMF code[17] to determine the phase diagram of equilibrium magnetic states in capped structures by modelling them as extruded hemispheres. This geometry considers the curvature-driven thickness gradient of the cap structures and provides further insight into the experimental findings.

The curvature template is obtained by dropcasting non-magnetic spherical silica particles (diameter: 50, 100, 330, 800 nm) onto a silicon wafer that results in an assembly of loosely distributed particles. The soft magnetic permalloy (Py, $Ni_{81}Fe_{19}$) film (20 nm) is deposited by means of dc-magnetron sputtering at room temperature (base pressure: 7×10^{-8} mbar; Ar pressure: 10^{-3} mbar). The magnetic film is sandwiched by a Ta capping (5 nm) and buffer (2 nm) layer. By positioning an aperture above the substrate, directional deposition with flux perpendicular to the sample surface is ensured. The resulting magnetic film exhibits a thickness gradient from top towards the equator due to the effectively varying deposition angle caused by the curvature.[14]

In order to image the magnetic domains in curved nanostructures, XMCD-PEEM[18] at the L_3 absorption edge of nickel is applied. In the used set-up, the polarized x-ray radiation hits the sample under an angle of $74°$ with respect to the surface normal. The XMCD-PEEM contrast reveals the magnetization parallel (red) and antiparallel (blue) to the direction of the x-ray beam. As a reference, the magnetic signal of a planar disk with a diameter of 300 nm on top of a substantially underetched pillow is depicted [Fig. 1(a)]. The location of disks and caps is indicated by dashed circles in Figs. 1(a)–1(c). For the planar disk, the well-known *dipolar* contrast appears that is characteristic for the curling of the in-plane magnetization of vortices.[19] In contrast, the magnetic signal of the cap structures with a diameter down to
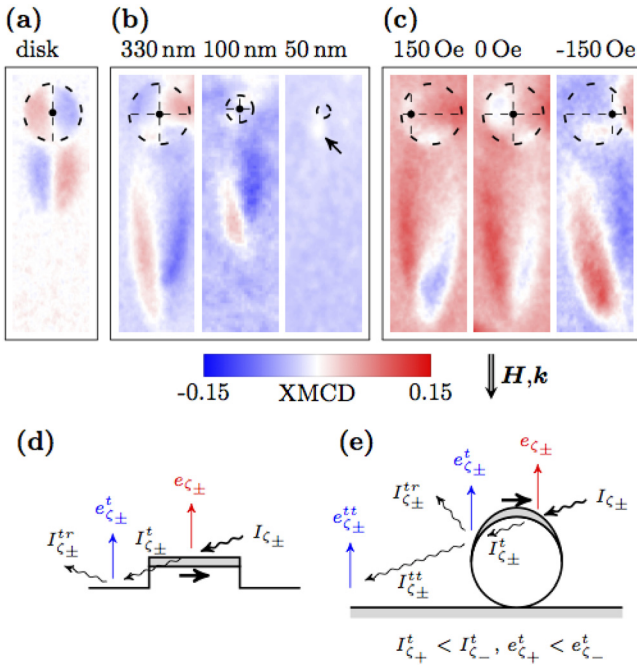
a)Electronic mail: r.streubel@ifw-dresden.de.

FIG. 1. (a) Magnetic vortex state in a planar disk ($\varnothing = 300\,\text{nm}$) on top of an underetched pillow visualized by XMCD-PEEM. (b) XMCD-PEEM signal of 20 nm thick Py caps with diameters of 330, 100, 50 nm (field of view: $350 \times 1200\,\text{nm}^2$). (c) Vortex core displacement causes a significant change of the tail contrast. Both samples show due to transmission an inverted tail contrast. The schematics illustrate the contrast origin of three-dimensional magnetic structures: (d) planar significantly underetched Py disk, and (e) Py cap.

100 nm exhibits at remanence a *quadrupole-like* pattern accompanied by an inverted tail contrast [Fig. 1(b)]. This tail contrast is also observed for underetched disks [Fig. 1(a)] and magnetic tubes.[20] A non-zero background contrast is apparent, because the surrounding planar substrate is also covered with the magnetic film. The peculiar appearance of the vortex state in cap structures was proven for caps with a diameter of 330 nm by applying an external magnetic field parallel (panel c, left image) or antiparallel (panel c, right image) to the direction of x-rays and detecting the displacement of the vortex core perpendicular to the field direction [Fig. 1(c)].

The origin of the quadrupole pattern and the tail contrast is related to the transmission effect of the x-ray radiation. In XMCD-PEEM, the magnetization component along the incidence plane is determined by the difference between the intensity of photoelectrons $e_{\zeta_\pm}$ emanated after exciting with left- and right-circular polarized light and normalized by their sum:

$$XMCD = \frac{e_{\zeta_+} - e_{\zeta_-}}{e_{\zeta_+} + e_{\zeta_-}}. \qquad (1)$$

Three-dimensional structures, which are partially transparent to x-ray radiation, exhibit due to the helicity-dependent absorption an inverted XMCD contrast in their shadow,[20] the tail contrast [left side in Figs. 1(d) and 1(e)]. In case of isolated spheres, the tail contrast is stretched along the incidence direction, which enhances the spatial resolution of the PEEM along this direction. For a sphere with a diameter of 330 nm under illumination at $74°$ with respect to the film normal, the expected shadow along the beam is about $1.2\,\mu\text{m}$, which agrees well with the experimental observa-

tion. In addition, the tail contrast suffers less from local field distortion caused by the sphere itself. This feature was experimentally proven by observing the magnetic vortex state in an underetched disk. The enhancement was further used to investigate the magnetic state of caps with a diameter of 50 nm [Fig. 1(b)]. Although no signal was detected from the cap structure, the monochrome tail contrast [indicated by an arrow in Fig. 1(b)] provided information about the onion state in the capped structure as revealed by numerical calculations.[14] Focusing on the tail contrast is also convenient for the investigation of small displacements of the vortex core [Fig. 1(c), core indicated by black point].

The obtained experimental data are compared to micromagnetic simulation carried out with the material parameters of Py.[21] The magnetic cap structure is modeled by an extruded hemisphere that has an inner and outer radius R and a constant thickness h [Fig. 2(a)]. This geometry accounts for the curvature-driven thickness gradient of the cap structures. We simulated the remanent states starting with different types of initial magnetization distributions: the uniform easy-axial state (along the cylinder axis), the uniform easy-plane one (along the cutting plane of the hemisphere), and the vortex distribution. All initial distributions lead to different locally stable curling states, corresponding to the energy minimum; while the global energy minimum is provided by the ground state. Following such a scheme, we constructed diagrams of equilibrium magnetization distribution [Fig. 2(b)]. The experimental data are indicated by double circles (red: vortex state, green: onion state), which agrees well with the theory. The importance of exploring the tail contrast is obvious, since otherwise no information could have been found about the boundary region.

In order to elucidate the phase diagram, it is instructive to use an analogy with a phase diagram of the planar disk.[16] Therefore, we overlaid the calculated diagram for caps with the boundaries of different phases of disk-shaped particles[22] [dashed lines in Fig. 2(b)]. The two phase diagrams are quite similar. However, there are differences, i.e., the monodomain state of the thin sample is almost uniform (in-plane flower
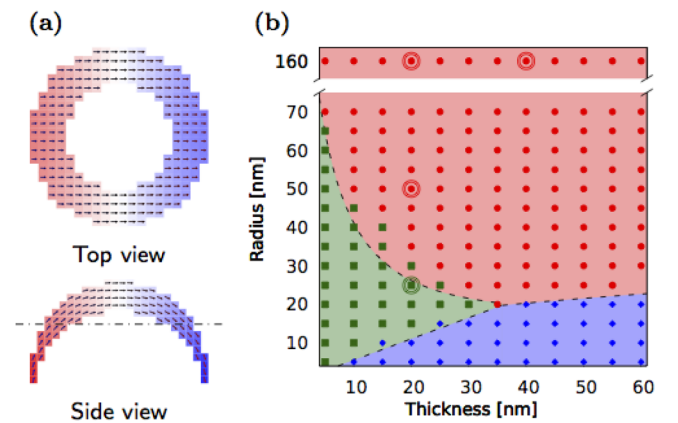

FIG. 2. (a) Magnetization distribution in a Py cap with a radius $R = 30\,\text{nm}$ and a thickness $h = 10\,\text{nm}$. The top view shows the cross-section as indicated in the side view. The sample is in the onion state. (b) Phase diagram of equilibrium magnetization states in caps. Symbols correspond to simulation data for Py nanocaps: ◆, uniform easy-axis state; ■, onion state; ●, vortex state; lines represent the phase boundaries of disks. The double circles indicate the experimental data.

state[16]) in case of the disk, while it is a curling state (onion state) in case of the caps. The reason is that the magnetization distribution of the onion state caps is close to uniform in the front view, while it is almost tangential in the side view [Fig. 2(a)]. Hence, the magnetostatic charges of the face surfaces are small, and the magnetostatic energy of such a cap is mainly due to the edge surface charges. Supposing that the magnetization is almost uniform in the xy-plane, we can use the approximation of the magnetization distribution in a uniformly magnetized disk.[22] For the vortex state, the magnetization distribution is similar to that of a planar disk. The boundary surface between two uniform states can be expressed analytically, $h = R\varepsilon_c$ with $\varepsilon_c \approx 1.47$.[23] When $\varepsilon < \varepsilon_c$ the magnetization lies in the xy-plane, while for $\varepsilon > \varepsilon_c$, the easy-axis state is favored.

In conclusion, we investigated the equilibrium magnetic states of soft magnetic cap structures. A way to enhance the spatial resolution of XMCD-PEEM by exploring the tail contrast instead of the structure contrast directly was presented. That way, we verified several points of the numerically calculated phase diagram for Py caps. Simulations were performed by considering capped structures as extruded hemispheres that account for the curvature-driven thickness gradient.

[1]R. P. Cowburn, D. K. Koltsov, A. O. Adeyeye, M. E. Welland, and D. M. Tricker, Phys. Rev. Lett. **83**, 1042 (1999).

[2]J. Stöhr and H. C. Siegmann, *Magnetism: From Fundamentals to Nanoscale Dynamics, Springer Series in Solid-State Sciences* Vol. 152 (Springer-Verlag, Berlin, 2006).

[3]J.-G. Zhu, Y. Zheng, and G. A. Prinz, J. Appl. Phys. **87**, 6668 (2000).

[4]R. P. Cowburn, J. Magn. Magn. Mater. **242–245**, 505 (2002).

[5]B. Van Waeyenberge, A. Puzic, H. Stoll, K. W. Chou, T. Tyliszczak, M. Fähnle, H. Brückl, K. Rott, G. Reiss, I. Neudecker, D. Weiss, C. H. Back, and G. Schütz, Nature (London) **444**, 461 (2006).

[6]K. Y. Guslienko, K.-S. Lee, and S.-K. Kim, Phys. Rev. Lett. **100**, 027203 (2008).

[7]B. Pigeau, G. de Loubens, O. Klein, A. Riegler, F. Lochner, G. Schmidt, and L. W. Molenkamp, Nat. Phys. **7**, 26 (2011).

[8]K. Yamada, S. Kasai, Y. Nakatani, K. Kobayashi, H. Kohno, A. Thiaville, and T. Ono, Nature Mater. **6**, 269 (2007).

[9]D. D. Sheka, Y. Gaididei, and F. G. Mertens, Appl. Phys. Lett. **91**, 082509 (2007).

[10]V. P. Kravchuk, D. D. Sheka, Y. Gaididei, and F. G. Mertens, J. Appl. Phys. **102**, 043908 (2007).

[11]V. P. Kravchuk, D. D. Sheka, R. Streubel, D. Makarov, O. G. Schmidt, and Y. Gaididei, Phys. Rev. B **85**, 144433 (2012).

[12]M. Albrecht, G. Hu, I. L. Guhr, T. C. Ulbrich, J. Boneberg, P. Leiderer, and G. Schatz, Nature Mater. **4**, 203 (2005).

[13]T. C. Ulbrich, D. Makarov, G. Hu, I. L. Guhr, D. Suess, T. Schrefl, and M. Albrecht, Phys. Rev. Lett. **96**, 077202 (2006).

[14]R. Streubel, D. Makarov, F. Kronast, V. Kravchuk, M. Albrecht, and O. G. Schmidt, Phys. Rev. B **85**, 174429 (2012).

[15]R. Streubel, D. J. Thurmer, D. Makarov, F. Kronast, T. Kosub, V. Kravchuk, D. D. Sheka, Y. Gaididei, R. Schäfer, and O. G. Schmidt, Nano Lett. **12**, 3961 (2012).

[16]C. A. Ross, M. Hwang, M. Shima, J. Y. Cheng, M. Farhoud, T. A. Savas, H. I. Smith, W. Schwarzacher, F. M. Ross, M. Redjdal, and F. B. Humphrey, Phys. Rev. B **65**, 144417 (2002).

[17]"The object oriented micromagnetic framework," developed by M. J. Donahue and D. Porter mainly, from NIST. We used the 3D version of the 1.2α4 release [http://math.nist.gov/oommf/].

[18]F. Kronast, J. Schlichting, F. Radu, S. Mishra, T. Noll, and H. Dürr, Surf. Interface Anal. **42**, 1532 (2010).

[19]S.-B. Choe, Y. Acremann, A. Schollm, A. Bauer, A. Doran, J. Stöhr, and H. A. Padmore, Science **304**, 420 (2004).

[20]J. Kimling, F. Kronast, S. Martens, T. Böhnert, M. Martens, J. Herrero-Albillos, L. Tati-Bismaths, U. Merkt, K. Nielsch, and G. Meier, Phys. Rev. B **84**, 174406 (2011).

[21]In all OOMMF simulation, we used the following material parameters of Py: exchange constant $A = 1.3 \times 10^{-11}$ J/m, saturation magnetization $M_S = 8.6 \times 10^5$ A/m, damping constant $\eta = 0.01$, on-site anisotropy was neglected and the cubic unit cell size was varied from 2.5 to 5 nm depending on the sample size.

[22]V. P. Kravchuk, D. D. Sheka, and Y. B. Gaididei, J. Magn. Magn. Mater. **310**, 116 (2007).

[23]See supplementary material at http://dx.doi.org/10.1063/1.4756708 for detailed theoretical derivation.